

ORIGINAL ARTICLE

Masayuki KITANO · Masatoshi KUDO  
Hiroki SAKAMOTO · Tatsuya NAKATANI  
Kiyoshi MAEKAWA · Nobuyuki MIZUGUCHI  
Yasuhiro ITO · Motohiro MIKI · Uwe MATSUI  
Tammo von SCHRENCK

## Preliminary study of contrast-enhanced harmonic endosonography with second-generation contrast agents

Received: April 19, 2007 / Accepted: September 4, 2007

### Abstract

**Purpose.** We developed a novel echoendoscope that enables contrast harmonic imaging using ultrasound contrast agents and performed contrast-enhanced harmonic endosonography (EUS) both in vitro and in vivo.

**Methods.** An experimental convex-array echoendoscope equipped with a wideband transducer and a specific mode for contrast harmonic imaging was used. A Doppler phantom model was employed in in vitro experiments to determine the optimal mechanical indices for contrast harmonic imaging by the echoendoscope. In the in vivo experiments, the echoendoscope was inserted into the stomachs of dogs. The digestive organs were observed after intravenous infusion of a contrast agent, Definity, using contrast-enhanced harmonic EUS. Two patients, one with pancreatic carcinoma and one with a gastrointestinal stromal tumor (GIST), underwent contrast-enhanced harmonic EUS.

**Results.** In vitro experiments revealed that the optimal mechanical indices were 0.35–0.40 for intermittent imaging and 0.30 or less for real-time imaging. In the in vivo experiments, branching vessels and subsequent homogeneous distribution of the signal in the pancreatic tissue were observed. During clinical application, typical vascular patterns were observed in pancreatic carcinoma and a GIST.

**Conclusion.** Contrast-enhanced harmonic EUS visualized parenchymal perfusion and the fine vascular structure in digestive organs and should be a useful and powerful method for clinical investigations.

**Keywords** contrast-enhanced harmonic endosonography · microcirculation

### Introduction

Contrast-enhanced harmonic imaging using an ultrasound contrast agent enables observation of the vasculature of the abdominal organs.<sup>1–16</sup> Endosonography (EUS) is an imaging modality with higher resolution than any other modality, including transabdominal ultrasonography.<sup>17,18</sup> However, to date, contrast harmonic imaging has been unavailable with EUS because of its limited band and low acoustic power. It has been shown that second-generation contrast agents produce harmonic signals at a low acoustic pressure,<sup>19–22</sup> and thus they may be suitable for EUS with a low acoustic pressure. We invented a novel echoendoscope equipped with a wideband transducer suitable for contrast-enhanced harmonic EUS. By means of this novel echoendoscope, we first attempted to determine the appropriate condition for detecting bubbles from a second-generation contrast agent, Definity (Astellas, Ibaraki, Japan), by phantom experiments, and subsequently used the system to observe the microcirculation of canine digestive organs in vivo after infusion of Definity.

### Materials and methods

#### Equipment

All experiments were conducted using a prototype convex-array echoendoscope equipped with a wideband transducer (Fig. 1). The radius of curvature, the center of the scanning frequency, and the scanning range of the transducer are 5 mm, 7.5 MHz, and 180°, respectively.

M. Kitano · M. Kudo · H. Sakamoto · T. Nakatani  
Division of Gastroenterology and Hepatology, Department of  
Internal Medicine, Kinki University School of Medicine,  
377-2 Ohno-Higashi, Osaka-Sayama 589-8511, Japan  
Tel. +81-72-366-0221 ext. 3525; Fax +81-72-367-2880  
e-mail: m-kitano@med.kindai.ac.jp

K. Maekawa  
Section of Abdominal Ultrasound, Kinki University School of  
Medicine, Osaka-Sayama, Japan

N. Mizuguchi  
Life Science Research Institute, Kinki University School of  
Medicine, Osaka-Sayama, Japan

Y. Ito · M. Miki  
Research and Development Department, Aloka Co. Ltd, Tokyo,  
Japan

U. Matsui · T. von Schrenck  
Department of Medicine, Bethesda General Hospital Bergedorf,  
Hamburg, Germany

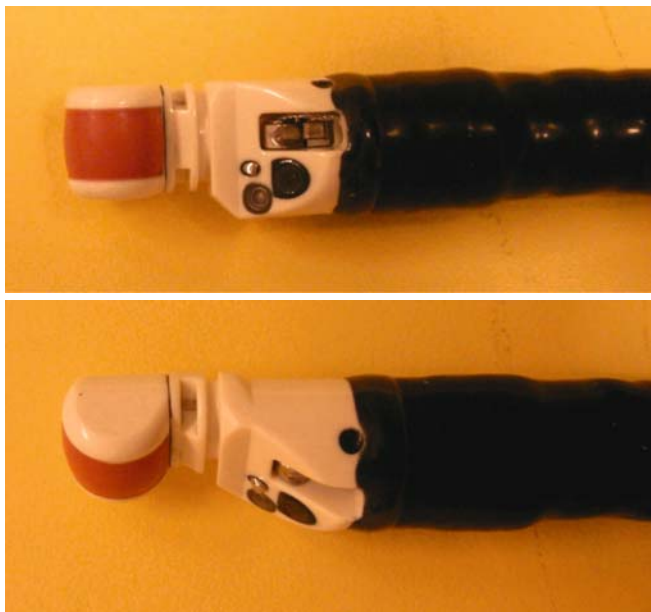


**Fig. 1.** Prototype echoendoscope equipped with a wideband transducer used in this study

Image analysis was performed using an Aloka ProSound-6500 (Aloka, Tokyo, Japan). Extended pure harmonic detection (ExPHD) mode, which is specific to contrast-enhanced harmonic ultrasonography, was employed. The principle of contrast-enhanced harmonic imaging based on ExPHD mode is described below. When the tissue and the microbubbles receive transmitted ultrasound waves, harmonic components that are integer multiples of the fundamental frequency are produced. The harmonic content derived from microbubbles is higher than that from tissues (Fig. 2). Ordinary contrast harmonic imaging more intensively depicts signals from the microbubbles than those from the tissue by selectively detecting the second harmonic components. However, ordinary contrast harmonic imaging is not able to filter the signals from the tissue. The ExPHD mode selectively depicts signals from the microbubbles, filtering those from the tissue by synthesizing the phase-shift signals with the second harmonic components (Fig. 2). Signals from the contrast agent vary greatly in phase, with no relation to its motion, when ultrasound pulses are transmitted multiple times. On the other hand, signals are hardly changed between multiple transmissions in the part without the contrast agent. ExPHD technology detects the relative phase shifts of the received signals by transmitting and receiving ultrasound beams multiple times on the same acoustic line (Fig. 2). Phase-shift signals output from the phase detection circuit are synthesized with second harmonic signals to reinforce the second harmonic signals (Fig. 2). This processing is capable of enhancing the imaging of signals from contrast agents. In ExPHD mode, the transmit frequency was 4.28 MHz and the receiving frequency band was the slightly lower part of the second harmonics. The gain and dynamic range were adjusted to avoid signal saturation.

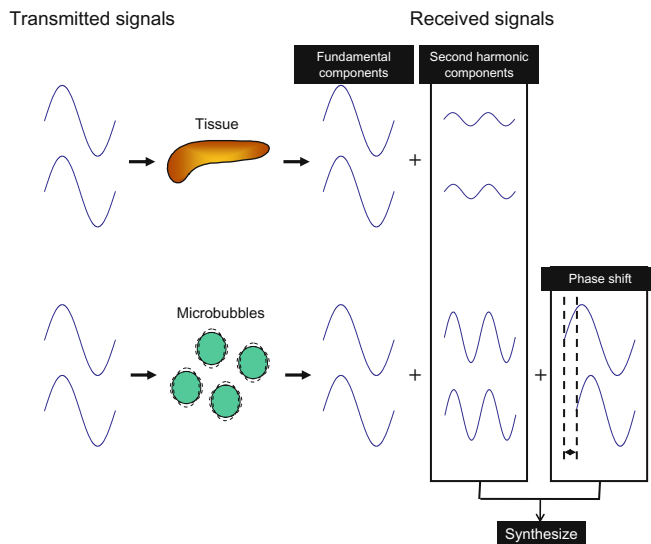


**Fig. 2.** Principle of extended pure harmonic detection (ExPHD) mode. The microbubbles produce stronger second harmonic signals as well as a greater phase shift than the tissue does. Contrast harmonic imaging based on the Extended pure harmonic detection (ExPHD) mode selectively depicts signals from contrast agents by synthesizing the phase-shift signals with the second harmonic components

## Drugs

Definity was provided by Astellas Pharmaceutical Co. Ltd. (Ibaraki, Japan). Immediately before use, Definity was shaken for 45 s to produce air bubbles.

## In vitro studies

Doppler phantom Model 524 (ATS, Bridgeport, CT, USA) and Doppler flow controller and pumping systems (ATS) were employed for phantom experiments. The Doppler phantom model consisted of urethane rubber with an attenuation coefficient of 0.5 dB/cm/MHz; it contains flow channels 8 mm in diameter located 15.0 mm below the scan surface. The chamber of the pumping system holds 2 l of saline. The experiments were performed according to the following procedure. First, the transmitting acoustic power was adjusted while freezing the image. The diluted solution of Definity (2.5  $\mu$ l/l and 5.0  $\mu$ l/l, diluted in saline) was stirred lightly and continuously in the chamber. Then, the flow channels of the phantom were perfused with the diluted solution of Definity using the pump. Subsequently, the flow of the solution of Definity was stopped for 10 s. The machine was unfrozen and image data were captured for 1 s (8 frames). The experiments were performed using different acoustic power (mechanical index) settings, i.e., from 0.18 to 0.66. Echo intensity inside and outside the flow channel was taken from the histogram of the regions of interest (Figs. 3,4) and expressed as a percentage of the maximal level. The change in echo intensity was expressed as the difference in echo intensity between the inside and the outside of the flow channels. The changes in echo intensity for the first frame and 1 s (8 frames) later between

**Fig. 3a-d.** Images of phantom experiments after the first frame for different condition settings. Echo intensity in the region of interest was measured as a percentage of the maximal level outside the tube (*upper framed area*) and inside the tube (*lower framed area*). The concentration of Definity and the mechanical index (MI) were, respectively, **a** 2.5  $\mu\text{l/l}$ , 0.18; **b** 2.5  $\mu\text{l/l}$ , 0.22; **c** 5.0  $\mu\text{l/l}$ , 0.22; **d** 5.0  $\mu\text{l/l}$ , 0.30. Arrowhead, focus point

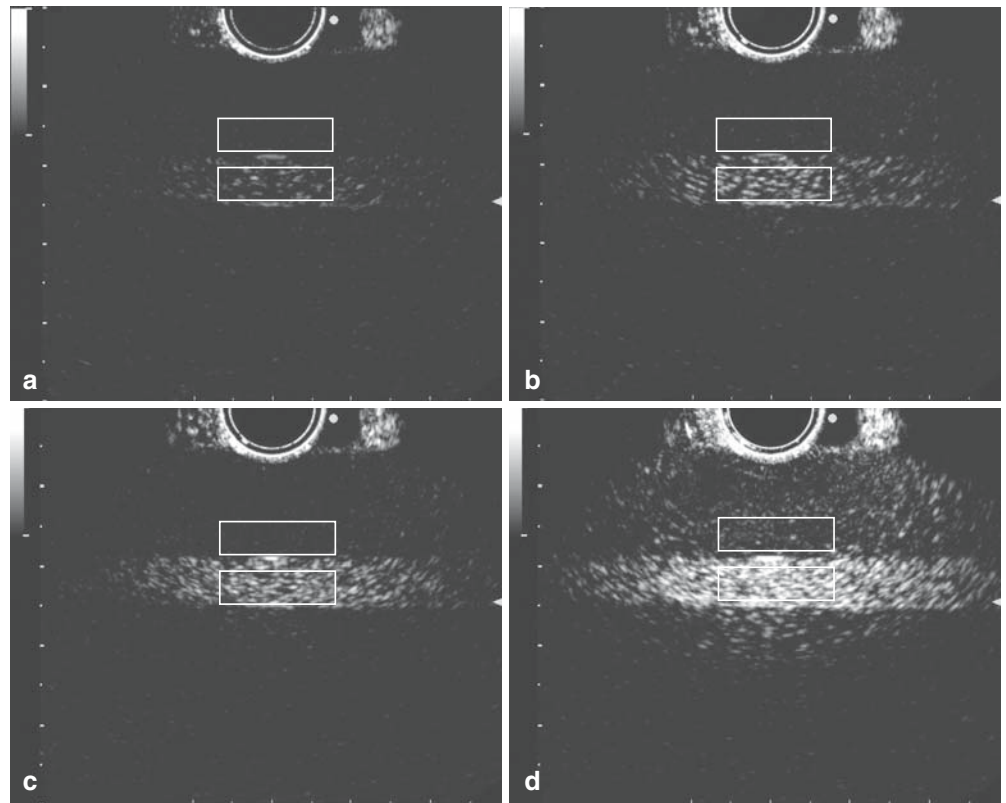
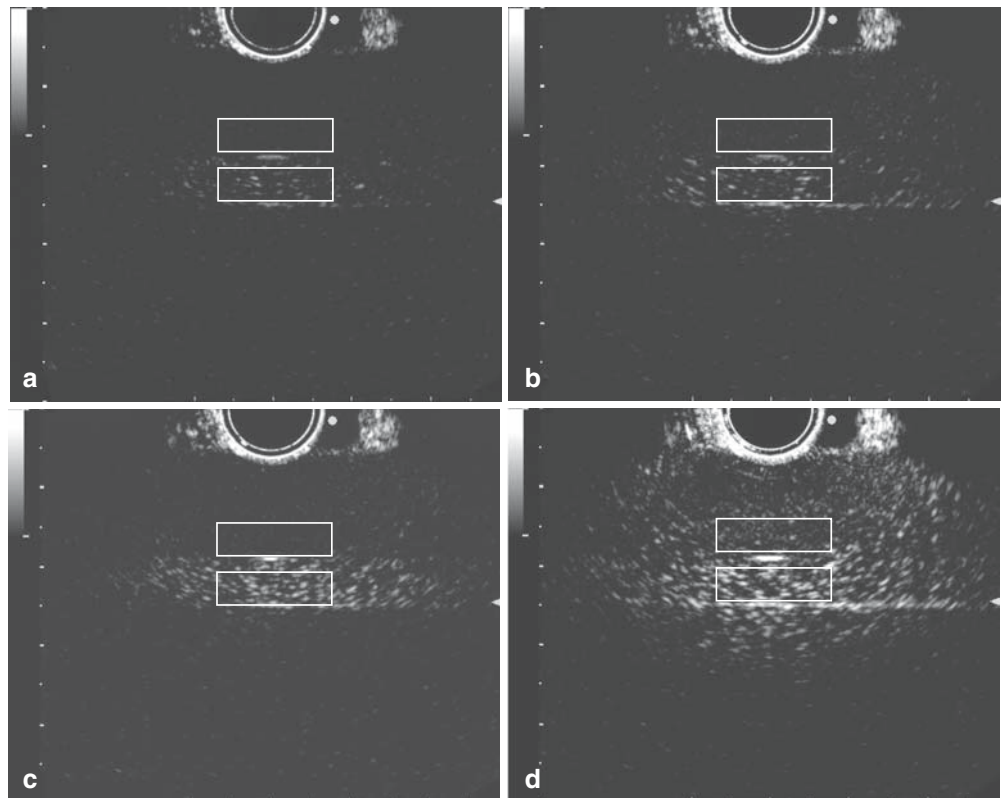


**Fig. 4a-d.** Images of the phantom experiment after transferring the signals 8 times/s for 1 s with different condition settings. Echo intensity in the region of interest was measured as a percentage of the maximal level outside the tube (*upper framed area*) and inside the tube (*lower framed area*). The concentration of Definity and the mechanical index (MI) were, respectively, **a** 2.5  $\mu\text{l/l}$ , 0.18; **b** 2.5  $\mu\text{l/l}$ , 0.22; **c** 5.0  $\mu\text{l/l}$ , 0.22; **d** 5.0  $\mu\text{l/l}$ , 0.30



the different mechanical indices were calculated and the optimal mechanical indices for depicting bubbles were determined.

### In vivo studies

Twelve male beagle dogs (9.5–10.5 kg) were used to carry out contrast-enhanced harmonic EUS. All experiments were performed under the guidelines of the National Research Council's *Guide for the Care and Use of Laboratory Animals*. The dogs were fasted for 24 h before the experiments. On the day of the procedure, the dogs were sedated with thiopental (20 mg/kg) and then intubated; anesthesia was maintained with pentobarbital (30 mg/h) and galamine (30 mg/h). After anesthesia, the dogs were mechanically ventilated. After completion of the anesthetization procedures, the prototype convex-array echoendoscope was inserted into the dogs' stomachs. The gastric wall, pancreas, and gallbladder were sequentially observed by EUS from the distal part of the gastric lumen. Prior to injection of Definity, a scanning plane displaying the pancreas was chosen on fundamental B-mode (10 MHz). After changing to ExPHD mode, a bolus of Definity (20  $\mu$ l/kg) was injected intravenously. The optimal mechanical index obtained in the in vitro study (0.24) was employed in the in vivo study. When the first signal appeared from the organs, images of the ideal scanning plane were displayed for about 60 s in a real-time continuous fashion.

After observing the organs, lesions were artificially produced in the stomach or the pancreas in order to estimate the accuracy of contrast-enhanced EUS. In six dogs, 1 ml of saline was injected into the gastric submucosa. A 22-G needle (Olympus NA-200H-8022, Olympus Medical Systems, Tokyo, Japan) was used to puncture the third layer (submucosal layer) using EUS images as a guide, and 1 ml of saline was injected into the layer. In the other six dogs, the abdomen was opened by midline incision. In order to estimate the accuracy of contrast-enhanced EUS, a pancreatic lesion was artificially produced by radiofrequency ablation. Radiofrequency ablation of the pancreas was performed using an RF generator and a LeVeen needle (RTC 2000, Radiotherapeutic, Sunny Vale, CA, USA). The electrode needle for radiofrequency ablation had a 25-cm-long stainless steel shaft insulated by a plastic membrane and 8–10 retractable lateral hooks with a maximum exposed deployment of 2.0 cm. The needle was inserted into the center of the pancreas. Subsequently, lateral hooks were extended from the steel shaft into the pancreas, and part of the pancreas was ablated. The emission power, tissue impedance value, and treatment time were displayed on the generator monitor. The initial emission power was set at 30 W. Then, the emission power was gradually increased to up to 60 W. The radiofrequency energy was applied for 12–15 min or was automatically stopped when power "roll-off" occurred. After the artificial lesions were made, they were observed using the procedure described above.

The dogs were killed by administration of an overdose of pentobarbital and the pancreas was immediately

removed; the maximal diameter of the ablated lesion in the pancreas was measured. Values for the maximal diameter of ablated lesions were compared with those of the perfusion defect determined by contrast-enhanced harmonic imaging.

### Clinical application

Contrast-enhanced harmonic EUS was performed on two patients, one with a pancreatic carcinoma and one with a gastrointestinal stromal tumor, after written informed consent had been obtained from them. A different echoendoscope from that used for dogs was employed for clinical usage. The shape, the material, and the condition settings of the echoendoscope were exactly the same as those used for dogs. The examinations were performed with the approval of the ethics committee of the Hamburg Chamber of Physicians.<sup>23</sup> After an abnormal lesion was detected in the pancreas or the stomach by fundamental B-mode EUS, the setting was changed to ExPHD mode. Observation was continued in a real-time fashion until 90 s after a bolus infusion of 2 ml SonoVue (Bracco Imaging, Milan, Italy).

## Results

### In vitro studies

With mechanical indices lower than 0.35, the changes in echo intensity at the first frame increased with the mechanical indices for both concentrations of Definity (2.5 and 5.0  $\mu$ l/l) (Figs. 3,5). They reached a maximum level with mechanical indices of 0.35–0.40 (Fig. 5). On the other hand, the changes in echo intensity after transferring the signals 8 times/s for 1 s increased in parallel with those at the first frame until mechanical indices of 0.24 and 0.30 were reached by perfusion of 2.5 and 5.0  $\mu$ l/l Definity, respectively (Figs. 4, 5). However, the changes in echo intensity were lowered by mechanical indices greater than 0.24 and 0.30 for 2.5 and 5.0  $\mu$ l/l Definity, respectively (Fig. 5).

### In vivo studies

#### *Gastric wall*

With fundamental B-mode EUS, the gastric wall in the dog consisted of five layers. With Extended pure harmonic detection (ExPHD) mode, signals appeared as transverse flow in the third layer and some perforating flow in the fourth layer (Fig. 6). Subsequently, signals appeared as vessels flowing in both directions between the serosal and luminal sides in the first and second layers (Fig. 6). The mucosal layer was diffusely stained by the signals 7–10 s later (Fig. 6). The area where saline was injected was free from echo signals with fundamental B-mode EUS (Fig. 7). With contrast-enhanced EUS, some vessel flow between the luminal and the serosal sides was observed in the echo-free space (Fig. 7).

**Fig. 5a,b.** Relationship between mechanical indices and changes in echo intensity after the first frame (1F) and after continuous transfer of signals (1 s later, 8F) on the Doppler phantom. Two concentrations of Definity were perfused into the phantom tube: **a** 2.5  $\mu\text{l/l}$ , **b** 5.0  $\mu\text{l/l}$

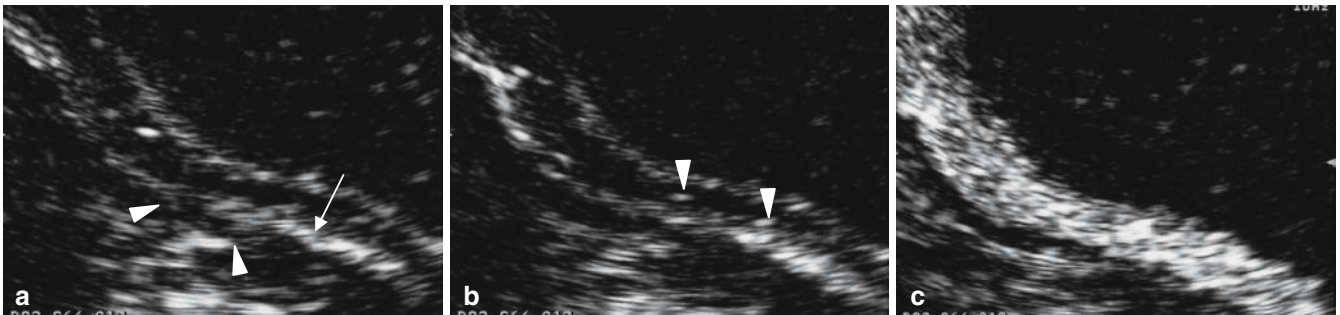
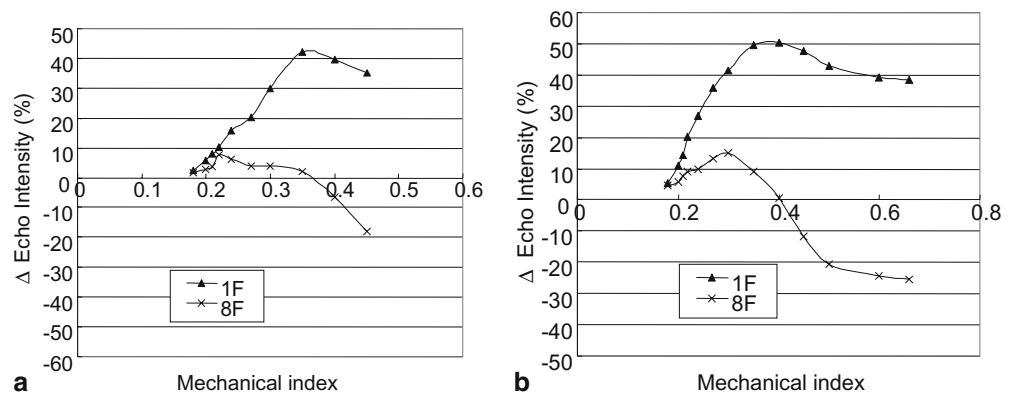


**Fig. 6a–c.** Contrast-enhanced harmonic imaging of the dog stomach. **a** Image of the gastric wall 4 s after infusion of Definity (20  $\mu\text{l/kg}$ ), in which perforating vessels through the fourth layer (proper muscle layer, *arrowheads*) are depicted. Vessels flowing transversely are visualized in the third layer (submucosal layer, *arrow*). **b** Image of the

gastric wall 5 s after infusion of Definity. In the first and second layers (mucosal layer), bidirectional flow between luminal and serosal sides is visualized (*arrowheads*). **c** Image of the gastric wall 7 s after infusion of Definity, showing homogeneous enhancement of the mucosal layer (the first and second layers)

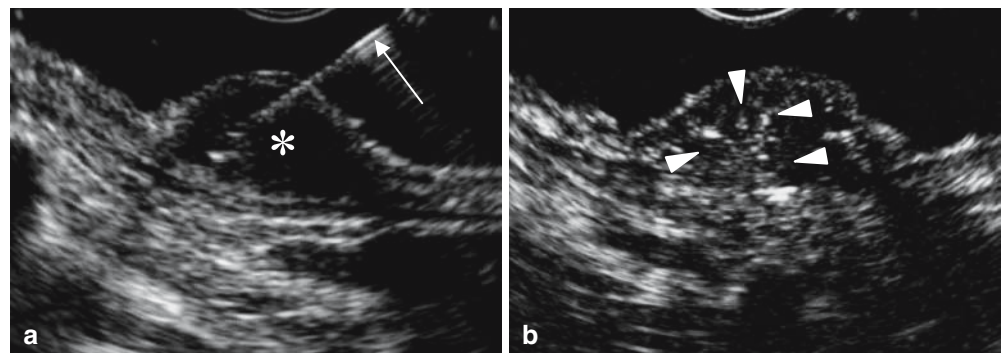


**Fig. 7a,b.** Imaging of the dog stomach following injection of saline into the submucosa. **a** Fundamental B-mode image of the saline-injected gastric wall. Saline was injected using a EUS guided fine needle aspiration (EUS-FNA) needle (*arrow*) into the third layer (submucosal

layer). An echo-free space was produced by the injection (*asterisk*). **b** Image of the gastric wall 20 s after infusion of Definity (20  $\mu\text{l/kg}$ ). Stretched vessels (*arrowheads*) are apparent between the luminal and serosal sides

### Pancreas

A total of 4–6 s after injection of Definity, contrast signals appeared at the periphery and around the main duct of the dog pancreas, and then branched off (Fig. 8); after 8–10 s, signals from the contrast agent were homogeneously distributed (Fig. 8). The macroscopic appearance of the ablated lesion was whiter in color compared to the surrounding tissue (Fig. 9). After radiofrequency ablation, the ablated

lesion was depicted as a low echoic area with a high echoic part with unclear margin (Fig. 9). The injection of Definity demonstrated that there were no or few vessels in the low echoic lesion and abundant vessels in the surrounding tissue (Fig. 9). The ablated area appeared as a perfusion defect, and the size of the hypovascular defect ( $13.7 \pm 4.2$  mm in diameter) closely mirrored the macroscopic appearance of the ablated lesion ( $14.5 \pm 3.4$  mm in diameter) ( $n = 6$ , Fig. 9a,c).

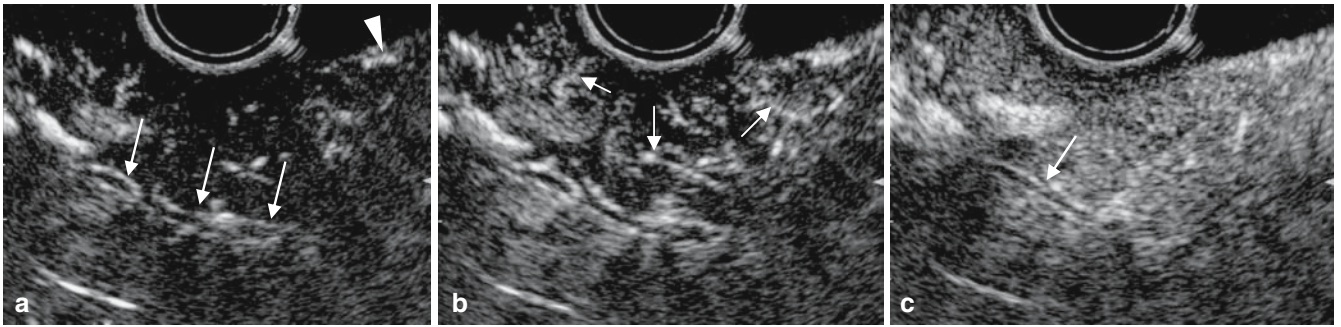


**Fig. 8a–c.** Contrast-enhanced harmonic imaging of the dog pancreas. **a** Image of the pancreas 5 s after infusion of Definity (20  $\mu$ l/kg). Signals from the microbubbles appeared around the main pancreatic duct (arrows) and in the surrounding vessels (arrowhead). **b** Image of the pancreas 6 s after infusion of Definity, in which vessels branching off into the pancreas (arrows) are apparent. **c** Image of the pancreas 10 s after infusion of Definity, showing homogeneous distribution of the signal. The main pancreatic duct is clearly delineated by the sharp contrast with the parenchyma (arrow)

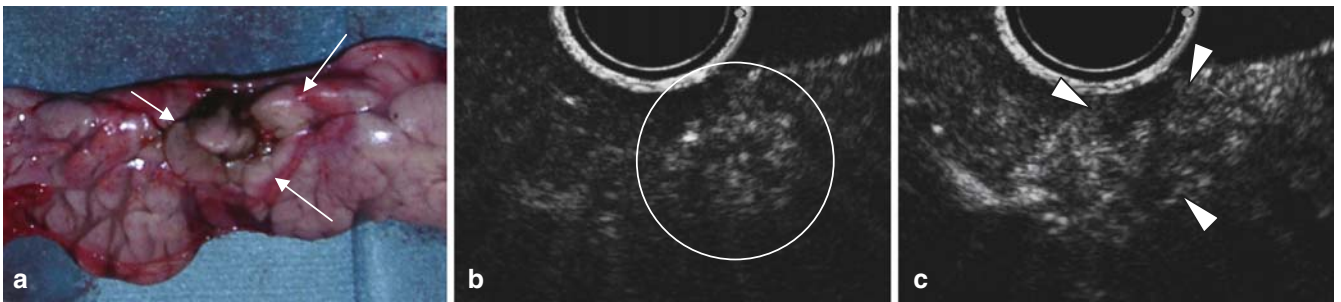


**Fig. 9a–c.** Contrast-enhanced harmonic imaging of the ablated pancreas. **a** Macroscopic appearance of the pancreatic lesion generated by radiofrequency ablation. A round, white-colored lesion (arrows) was observed in the ablated area. **b** Image of the pancreas immediately before infusion of Definity (20  $\mu$ l/kg). An obscure high echoic area was observed in the ablated area (circle). **c** Image of the pancreas 20 s after infusion of Definity. The ablated area was evident as a perfusion defect (arrowheads)

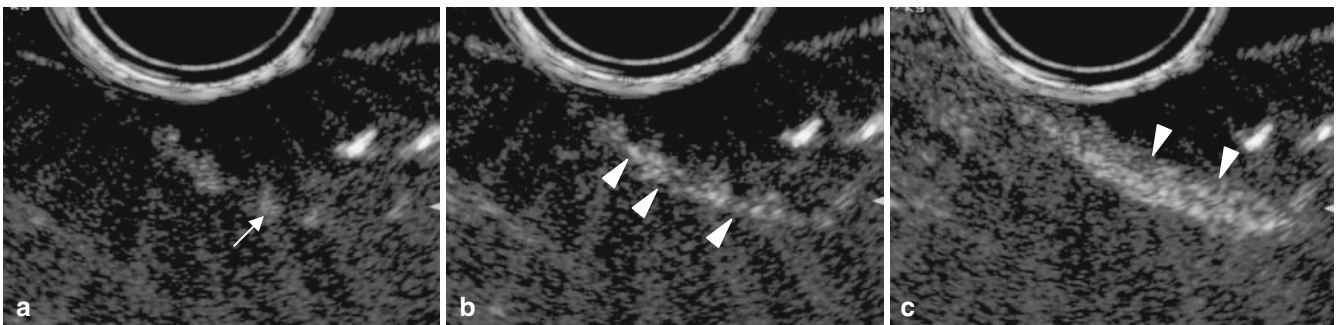


**Fig. 10a–c.** Contrast-enhanced harmonic imaging of the gallbladder wall in a dog. **a** Image of the gallbladder 3 s after infusion of Definity (20  $\mu$ l/kg). Some vessels flowing into the gallbladder have started to appear (arrow). **b** Image of the gallbladder 4 s after infusion of Definity showing the outer layer (arrowheads). **c** Image of the gallbladder 6 s after infusion of Definity, showing the inner layer (arrowheads)

### Gallbladder

After injection of Definity, the signals of the contrast agent appeared around the gallbladder. Subsequently, the outer and the inner layers were sequentially resolved by contrast-enhanced EUS (Fig. 10).

### Clinical application

In the patient with a pancreatic carcinoma, fundamental B-mode EUS revealed a low echoic tumor at the pancreatic tail (Fig. 11). Contrast-enhanced EUS showed no vessels in the tumor, whereas the splenic artery was strongly enhanced

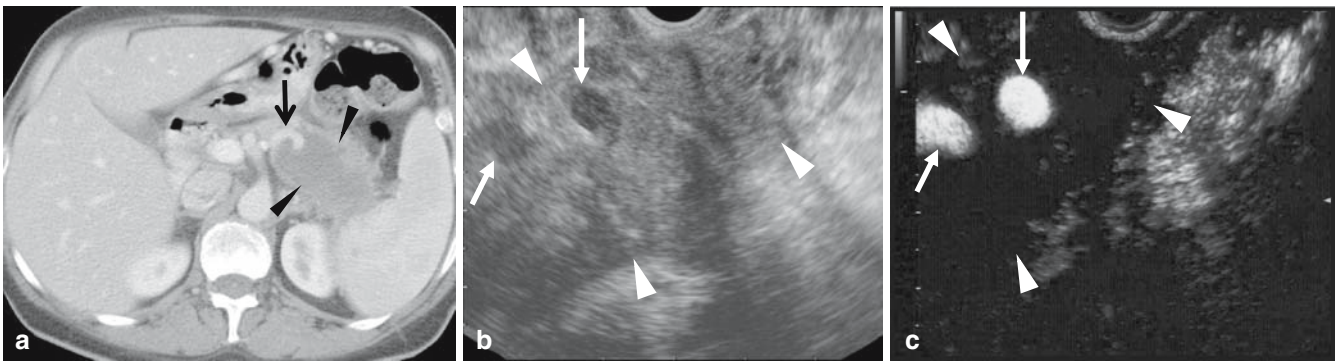


**Fig. 11a–c.** Imaging of a pancreatic carcinoma. **a** Image on contrast-enhanced computed tomography. Contrast-enhanced computed tomography shows a tumor with low density (*arrowheads*) at the pancreatic tail. The *arrow* indicates the splenic artery. **b** Image using fundamental B-mode. A low echoic tumor 4 cm in maximal diameter

(*arrowheads*) is observed at the pancreatic tail. *Arrows* show the splenic artery. **c** Image using ExPHD mode. No vascular signals are observed in the tumor (*arrowheads*), although the splenic artery (*arrows*) is enhanced

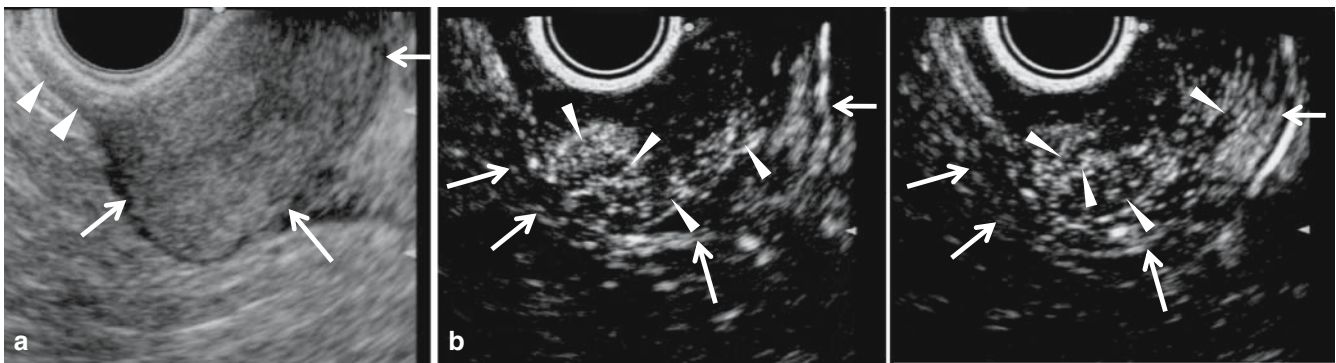


**Fig. 12a,b.** Imaging of a gastrointestinal stromal tumor of the stomach. **a** Image using fundamental B-mode. An oval tumor 3 cm in diameter (*arrows*) contiguous to the fourth layer (*arrowheads*) of the gastric wall

is observed. **b** Images using ExPHD mode. Diffuse fine vascular structure (*arrowheads*) is visualized over the tumor (*arrows*)

(Fig. 11). This vascular structure was consistent with that shown on contrast-enhanced computed tomography (Fig. 11). In the patient with a gastrointestinal stromal tumor, fundamental B-mode EUS showed an oval tumor contiguous to the fourth layer of the gastric wall. Diffuse fine vessels were clearly visualized over the tumor in a real-time fashion by contrast-enhanced EUS (Fig. 12).

## Discussion

A wide variety of ultrasound (US) contrast agents for intravenous infusion have been developed, and the use of microbubble agents such as Levovist, Albunex, and Optison have been shown to enable visualization of slow flow in fine vessels and characterization of tumor vascularity in color- or power-Doppler studies using EUS.<sup>24–31</sup> However, there are several limitations to ultrasound contrast agents in Doppler US studies, e.g., blooming artifacts, poor spatial resolution, and low sensitivity to slow flow. In the present study, we first attempted to visualize contrast harmonic images of digestive organs using a prototype echoendoscope equipped with a wideband transducer, which is suited to contrast harmonic imaging using a second-generation

contrast agent. In *in vitro* experiments, we attempted to determine the optimal mechanical indices for obtaining signals from microbubbles. The changes in echo intensity at the first frame reached maximum level with mechanical indices of 0.35–0.40, which were regarded to be appropriate for producing parenchymal perfusion images with intermittent imaging. On the other hand, the changes in echo intensity after transferring the signals 8 times/s for 1 s reached maximum level with mechanical indices of 0.24–0.30. However, they were lowered by mechanical indices greater than 0.24 and 0.30 for 2.5 and 5  $\mu$ l/l Definity, respectively. These results suggest that the optimal mechanical indices for observing vessel images by real-time continuous imaging at 8 Hz are in the range 0.24–0.30. Based on these results, we observed digestive organs in a real-time fashion using a mechanical index lower than 0.30. Under these conditions, we succeeded in observing fine vessels in digestive organs by means of EUS with a prototype transducer. This method prevented artifacts such as blooming and overpainting that are seen with power Doppler US. In the pancreas, parenchymal vasculature was observed. In addition, it was possible to demonstrate that the area of lesions produced after radiofrequency ablation had no blood flow. The ablated area was clearly depicted as a perfusion defect, which closely correlated with the histological findings. In the stomach and

gallbladder, the characteristic microcirculation for each layer was observed. Interestingly, stretched vessels were visualized in the area injected with saline. These results indicate that contrast-enhanced harmonic EUS could play an important role not only in differential diagnosis but also in evaluation of the pathophysiological conditions of digestive diseases.

In clinical application, contrast-enhanced EUS was performed in two patients, one with a pancreatic carcinoma and one with a gastrointestinal stromal tumor. In the patient with a pancreatic carcinoma, the splenic artery was strongly enhanced, whereas no vessels were observed in the tumor, which was consistent with images from contrast-enhanced computed tomography. In the patient with a gastrointestinal stromal tumor, diffuse fine vessels were observed over the tumor. These results suggest that evaluation of vascularity by contrast-enhanced EUS may apply to clinical investigations for digestive diseases, such as gastrointestinal submucosal tumors and pancreatic carcinomas.

In conclusion, contrast-enhanced harmonic EUS is a useful modality for depicting the microcirculation of digestive organs. Further studies on patients with digestive diseases will be necessary to further substantiate the conclusions of this study.

**Acknowledgments** The present study was supported by grants from the Research and Development Committee Program of The Japan Society of Ultrasonics in Medicine, the Japan Society for the Promotion of Science, and the Japanese Foundation for Research and Promotion of Endoscopy.

## References

- Ding H, Kudo M, Onda H, et al. Evaluation of post-treatment response of hepatocellular carcinoma with contrast-enhanced coded phase-inversion harmonic US: comparison with dynamic CT. *Radiology* 2001;221:721–30.
- Oshikawa O, Tanaka S, Ioka T, et al. Dynamic sonography of pancreatic tumors: comparison with dynamic CT. *AJR* 2002;178:1133–7.
- Kudo M. Contrast harmonic imaging in the diagnosis and treatment of hepatic tumors. Tokyo: Springer; 2003.
- Minami Y, Kudo M, Kawasaki T, et al. Evaluation of the effectiveness of transcatheter arterial chemoembolization for hepatocellular carcinoma: value of coded phase-inversion harmonics. *AJR* 2003;180:703–8.
- Nagase M, Furuse J, Ishii H, Yoshino M. Evaluation of contrast enhancement patterns in pancreatic tumors by coded harmonic sonographic imaging with a microbubble contrast agent. *J Ultrasound Med* 2003;22:789–95.
- Takeda K, Goto H, Hirooka Y, et al. Contrast-enhanced transabdominal ultrasonography in the diagnosis of pancreatic mass lesions. *Acta Radiologica* 2003;44:103–6.
- Wen YL, Kudo M, Minami Y, et al. Radiofrequency ablation of hepatocellular carcinoma: therapeutic response using contrast-enhanced coded phase-inversion harmonic sonography. *AJR* 2003;181:57–63.
- Kitano M, Kudo M, Maekawa K, et al. Dynamic imaging of pancreatic diseases by contrast-enhanced coded phase-inversion harmonic ultrasonography. *Gut* 2004;53:854–9.
- Minami Y, Kudo M, Kawasaki T, et al. Percutaneous radiofrequency ablation guided by contrast-enhanced harmonic sonography with artificial pleural effusion for hepatocellular carcinoma in the hepatic dome. *AJR* 2004;182:1224–6.
- Ohshima T, Yamaguchi T, Ishihara T, et al. Evaluation of blood flow in pancreatic ductal carcinoma using contrast-enhanced, wide band Doppler ultrasonography: correlation with tumor characteristics and vascular endothelial growth factor. *Pancreas* 2004;28:335–43.
- Wen YL, Kudo M, Zheng RQ, et al. Characterization of hepatic tumors: value of contrast-enhanced coded phase inversion harmonic US. *AJR* 2004;182:1019–26.
- Masaki T, Ohkawa S, Amano A, et al. Noninvasive assessment of tumor vascularity by contrast-enhanced ultrasonography and the prognosis of patients with nonresectable pancreatic carcinoma. *Cancer* 2005;103:1026–35.
- Fukuta N, Kitano M, Maekawa K, et al. Estimation of the malignant potential of gastrointestinal stromal tumors: the value of contrast-enhanced coded phase-inversion harmonic US. *J Gastroenterol* 2005;40:247–55.
- Numata K, Ozawa Y, Kobayashi N, et al. Contrast-enhanced sonography of pancreatic carcinoma: correlations with pathological findings. *J Gastroenterol* 2005;40:631–40.
- Sofuni A, Iijima H, Moriyasu F, et al. Differential diagnosis of pancreatic tumors using contrast imaging. *J Gastroenterol* 2005;40:518–25.
- Inoue T, Kitano M, Kudo M, et al. Diagnosis of gallbladder diseases by contrast-enhanced phase-inversion harmonic ultrasonography. *Ultrasound Med Biol* 2007;33:353–61.
- Zuccaro G, Sterling MJ. Endosonography in pancreatic disease: differential diagnosis. In: van Dam J, Svak MV, editors. *Gastrointestinal endoscopy*. New York: Saunders; 1999. p. 235–43.
- DeWitt J, Devereaux B, Chriswell M, et al. Comparison of endoscopic ultrasonography and multidetector computed tomography for detecting and staging pancreatic cancer. *Ann Intern Med* 2004;141:753–63.
- Gorce JM, Arditi M, Schneider M. Influence of bubble size distribution on the echogenicity of ultrasound agents. *Invest Radiol* 2000;35:661–71.
- Baert AL, Sartor K. Contrast media in ultrasonography. Basic principles and clinical applications. Berlin: Springer; 2005.
- Rickes S, Mönkemüller K, Malferteiner P. Echo-enhanced ultrasonography with pulse inversion imaging: a new imaging modality for the differentiation of cystic pancreatic tumours. *World J Gastroenterol* 2006;14:2205–8.
- Rickes S, Uhle C, Kahl S, et al. Echo enhanced ultrasound; a new valid initial imaging approach for severe acute pancreatitis. *Gut* 2006;53:74–8.
- Kimbel KH. Regulation of ethics committees in Germany. *Lancet* 1994;344:398.
- Ueno N, Tomiyama T, Tano S. Contrast-enhanced color Doppler ultrasonography in diagnosis of pancreatic tumor: two case reports. *J Ultrasound Med* 1996;15:527–30.
- Bhutani MS, Hoffman BJ, Velse A, Hawes RH. Contrast-enhanced endoscopic ultrasonography with galactose microparticles: SHU508A (Levovist). *Endoscopy* 1997;29:635–9.
- Hirooka Y, Naitoh Y, Goto H, et al. Usefulness of contrast-enhanced endoscopic ultrasonography with intravenous injection of sonicated serum albumin. *Gastrointest Endosc* 1997;46:166–9.
- Hirooka Y, Goto H, Itoh A, et al. Contrast-enhanced endoscopic ultrasonography in pancreatic diseases: a preliminary study. *Am J Gastroenterol* 1998;93:632–5.
- Becker D, Strobel D, Bernatik T, Hahn EG. Echo-enhanced color- and power-Doppler EUS for the discrimination between focal pancreatitis and pancreatic carcinoma. *Gastrointest Endosc* 2001;53:784–9.
- Hocke M, Schulze E, Gottschalk P, et al. Contrast-enhanced endoscopic ultrasound in discrimination between focal pancreatitis and pancreatic cancer. *World J Gastroenterol* 2006;12:46–50.
- Kanamori A, Hirooka Y, Itoh A, et al. Usefulness of contrast-enhanced endoscopic ultrasonography in the differentiation between malignant and benign lymphadenopathy. *Am J Gastroenterol* 2006;10:45–51.
- Săftoiu A, Popescu C, Cazacu S, et al. Power Doppler endoscopic ultrasonography for the differential diagnosis between pancreatic cancer and pseudotumoral chronic pancreatitis. *J Ultrasound Med* 2006;25:363–72.